
# Finite element simulation of noise radiation through shear layers

A. Prinn[a], G. Gabard[a] and H. Beriot[b]

[a]ISVR, University of Southampton, University Road, SO17 1BJ Southampton, UK
[b]LMS International - Leuven, LMS International Researchpark Haasrode ZI Interleuvenlaan 68 3001 Leuven
agp1g08@soton.ac.uk

Predicting sound propagation through the jet exhaust of an aero-engine presents the specific difficulty of representing the refraction effect of the mean flow shear. This is described in full in the linearised Euler equations but this model remains rather expensive to solve numerically. The other model commonly used in industry, the linearised potential theory, is faster to solve but needs to be modified to represent a shear layer. This paper presents a way to describe a vortex sheet in a finite element model based on the linearised potential theory. The key issues to address are the continuity of pressure and displacement that have to be enforced across the vortex sheet, as well as the implementation of the Kutta condition at the nozzle lip. Validation results are presented by comparison with analytical results. It is shown that the discretization of the continuity conditions is crucial to obtain a robust and accurate numerical model.

# 1 Introduction

This paper is concerned with the prediction of sound radiation from jet exhausts. An important aspect of such problems is the refraction of the sound waves by the mean flow shear as they propagate through the jet shear layer. This has a significant effect on the directivity of the sound radiated to the far field.

Another important aspect is that the sound field radiation is coupled at the trailing edge of the duct (or nozzle) to the vorticity shedding. This can also have a significant effect on sound radiation and requires an accurate description of the shed vorticity.

The Linearized Euler Equations (LEE) describe the propagation of linear disturbances in a steady inviscid mean flow, and include all the effects mentioned above. This model not only describes the sound waves but also includes the hydrodynamic and entropy waves. The downside is that the LEE are relatively costly to solve due to the large number of variables involved (4 or 5 in two- or three-dimensions). Another approach is to use the linearized potential theory which is based on the assumption that the mean flow and the perturbations derive from scalar potentials. This has the advantage of significantly reducing the cost of computational predictions, but the restriction placed on the mean flow excludes the case of jet exhausts, i.e. the shear layers cannot be represented by a potential flow assumption. This limitation can be addressed by constructing a model for a vortex sheet that represents the jet shear layer explicitly. This provides a good compromise between accuracy and computational efficiency.

The linearized potential theory is generally solved using finite element methods in the frequency domain [1] (but time-domain formulations have also been used), and this paper follows this approach. Two finite element formulations of the vortex sheet model have been proposed for the potential theory, by Eversman and Okunbor [3] and by Manera *et al.* [5]. The aim of this work was to revisit these models and to perform a quantitative assessment by comparing against an analytical solution for an idealized benchmark problem. This has lead to a new finite element formulation of the vortex sheet model which is able to accurately capture both the sound radiation and the vorticity shedding.

The problem of sound waves interacting with a vortex sheet separating two different mean flows is introduced in section 2. The finite element models are then presented in section 3. The results obtained with these models are compared against the analytical solution in section 4, first for uniform flows and then for non-uniform flows.

# 2 Problem description

We will work in the frequency domain using an $e^{+\mathrm{i}\omega t}$ notation. The propagation of small acoustic disturbances in a potential steady flow is described by the velocity potential $\phi$:

$$\mathrm{i}\omega\left(-\frac{\rho_0}{c_0^2}\frac{\mathrm{d}_0\phi}{\mathrm{d}t}\right)+\nabla\cdot\left(\rho_0\nabla\phi-\frac{\rho_0}{c_0^2}\frac{\mathrm{d}_0\phi}{\mathrm{d}t}\mathbf{u}_0\right)=0\,, \qquad (1)$$

where $\rho_0$, $c_0$ and $\mathbf{u}_0$ are the mean flow density, sound speed and velocity, and $\mathrm{d}_0/\mathrm{d}t = \mathrm{i}\omega+\mathbf{u}_0\cdot\nabla$ is the material derivative in the mean flow.

We consider that we have two different flow regions $\Omega_1$ and $\Omega_2$ separated by a vortex sheet $\Gamma$. The flow properties in each region are denoted by a subscript 1 or 2. On $\Gamma$ the mean flow is tangential: $\mathbf{u}_{01}\cdot\mathbf{n}=\mathbf{u}_{02}\cdot\mathbf{n}=0$, where $\mathbf{n}$ is the unit normal to $\Gamma$ pointing into $\Omega_2$. The solutions on either side of the vortex sheet are coupled by imposing kinematic and dynamic conditions [8]. They correspond to the continuity of normal acoustic displacement and pressure. The latter can be written as follows:

$$-\rho_{01}\frac{\mathrm{d}_{01}\phi_1}{\mathrm{d}t}=-\rho_{02}\frac{\mathrm{d}_{02}\phi_2}{\mathrm{d}t}\,,\quad \text{on } \Gamma, \qquad (2)$$

To formulate the continuity of the normal displacement $\xi$ one has to introduce this quantity as an independent variable in the model:

$$\frac{\mathrm{d}_{01}\xi}{\mathrm{d}t}=\frac{\partial\phi_1}{\partial n}\,,\quad \frac{\mathrm{d}_{02}\xi}{\mathrm{d}t}=\frac{\partial\phi_2}{\partial n}\,. \qquad (3)$$

An alternative to (3) is to impose the continuity of acoustic normal velocity. This can be written in terms of the velocity potential as follows:

$$\frac{\partial\phi_1}{\partial n}=\frac{\partial\phi_2}{\partial n}\,. \qquad (4)$$

To compare and validate the different finite element implementations of this model, we will consider a simplified test case of a circular straight duct, as illustrated in Figure 1. The duct extends from $z=0$ to $-\infty$ and its radius is $R$. In the cylindrical jet column ($r<R$) the mean flow is assumed uniform, and the same applies for the ambient mean flow ($r>R$). The mean flow properties can be different between these two regions. The vortex sheet is located at $r=R$ and originates from the duct trailing edge at $z=0$ and extends to $+\infty$. The source of sound is an acoustic mode propagating from within the duct to the far field. An analytical solution is available for this test case [4] based on the continuity of the acoustic displacement. It allows to calculate all quantities of interest in the near field (velocity potential, pressure, displacement, etc).

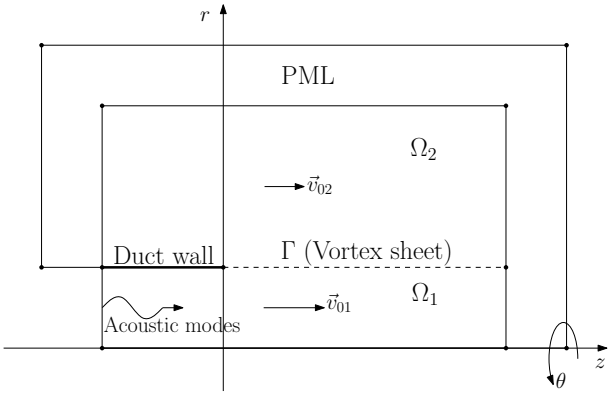


Figure 1: Schematic of the benchmark problem.

# 3 Finite element models

Equation (1) is solved using a standard finite element method based on the following variational formulation:

$$\int_\Omega \frac{\overline{\mathrm{d}_0 W}}{\mathrm{d}t}\frac{\mathrm{d}_0\phi}{\mathrm{d}t} - \nabla\overline{W}\cdot\nabla\phi\,\mathrm{d}\Omega + \int_{\partial\Omega}\overline{W}\mathbf{u}_0\cdot\mathbf{n}\frac{\mathrm{d}_0\phi}{\mathrm{d}t} - \overline{W}\frac{\partial\phi}{\partial n}\,\mathrm{d}S = 0\,,$$

where the overbar denotes the complex conjugate and $W$ is a test function. This formulation is applied to each acoustic domain $\Omega_1$ and $\Omega_2$. The integral on $\partial\Omega$ is modified to incorporate the appropriate boundary conditions. We will concentrate on the implementation of the vortex sheet at the surface $\Gamma$. Since the mean flow is parallel to the vortex sheet, the relevant terms in the variational formulation are:

$$\int_\Gamma \overline{W_1}\frac{\partial\phi_1}{\partial n} - \overline{W_2}\frac{\partial\phi_2}{\partial n}\,\mathrm{d}\Gamma\,.$$

## 3.1 Existing formulations of the vortex sheet

The formulation by Eversman and Okunbor [3] relies on the continuity of pressure and normal velocity, i.e. Equations (2) and (4). The normal displacement $\xi$ is still used as an independent variable on the vortex sheet $\Gamma$, and the associated test function is denoted by $\eta$. The displacement is related to the gradient of potential by

$$\mathrm{i}\omega\xi = \frac{\partial\phi_1}{\partial r} = \frac{\partial\phi_2}{\partial r}\,. \tag{5}$$

In addition the pressure continuity equation (2) is discretized using $\eta$ as the test function. Therefore, the relevant terms in the variational formulation are:

$$\int_\Gamma \overline{(W_1 - W_2)}\mathrm{i}\omega\xi + \overline{\eta}\left(\rho_{01}\frac{\mathrm{d}_{01}\phi_1}{\mathrm{d}t} - \rho_{02}\frac{\mathrm{d}_{02}\phi_2}{\mathrm{d}t}\right)\mathrm{d}\Gamma\,.$$

Eversman and Okunbor suggest that the test function $\eta$ should be constructed by taking the material derivative of the standard finite element shape function. This is equivalent to using

$$\int_\Gamma \overline{(W_1 - W_2)}\mathrm{i}\omega\xi + \overline{\frac{\mathrm{d}_0\eta}{\mathrm{d}t}}\left(\rho_{01}\frac{\mathrm{d}_{01}\phi_1}{\mathrm{d}t} - \rho_{02}\frac{\mathrm{d}_{02}\phi_2}{\mathrm{d}t}\right)\mathrm{d}\Gamma\,,$$

where standard shape functions are used for $\eta$.

Another alternative was proposed by Manera *et al.* [5] and it uses the continuity of displacement (3) instead of (5). The corresponding variational formulation is

$$\int_\Gamma \overline{W_1}\frac{\mathrm{d}_{01}\xi}{\mathrm{d}t} - \overline{W_2}\frac{\mathrm{d}_{02}\xi}{\mathrm{d}t} + \overline{\eta}\left(\rho_{01}\frac{\mathrm{d}_{01}\phi_1}{\mathrm{d}t} - \rho_{02}\frac{\mathrm{d}_{02}\phi_2}{\mathrm{d}t}\right)\mathrm{d}\Gamma\,.$$

In that context $\eta$ can be interpreted as a Lagrange multiplier which is used to impose the additional constraint that pressure should be continuous across the vortex sheet. Note that in both these formulations there is no attempt to control the behaviour of the solution at the trailing edge to satisfy the Kutta condition.

## 3.2 Proposed formulation

The new formulation is also based on the continuity of pressure and normal displacement, since these are the accepted matching conditions across the vortex sheet. In addition, it attempts to provide an explicit description of the Kutta condition at the trailing edge. To that end we also introduce the normal velocity on the vortex sheet as an independent variable. Note that two velocities are defined since this quantity is not necessarily continuous across the vortex sheet. These additional variables only represent a very small increase in the total number of degrees of freedom in the numerical model. We define the velocities as follows

$$v_1 = \frac{\mathrm{d}_{01}\xi}{\mathrm{d}t}\,,\quad v_2 = \frac{\mathrm{d}_{02}\xi}{\mathrm{d}t}\,,\ \text{on}\ \Gamma\,. \tag{6}$$

The test functions associated with the new variables $v_1$ and $v_2$ are denoted by $\sigma_1$ and $\sigma_2$. Equation (2) for the continuity of pressure is still discretized using $\eta$ as the test function. The advantage of having the displacement as an explicit variable is that one can directly impose the Kutta condition by setting $v_1 = v_2 = 0$ at the trailing edge.

The other element of novelty in the proposed formulation is the use of a Streamwise Upwind Petrov Galerkin (SUPG) method to discretize equations (2) and (6). This can be justified by noting that the oscillations of the vortex sheet will be caused not only by acoustic waves propagating through it but also by the vorticity shedding from the trailing edge. The latter is hydrodynamic in nature and has quite different properties from the acoustic field. In particular its wavelength is smaller and given by $\omega/u_0$ (there is therefore a factor $M$ between the acoustic and hydrodynamic wavelengths). These hydrodynamic oscillations are simply convected by the mean flow along the vortex sheet. It is well-known that standard finite elements are particularly inefficient at representing such solutions due to the lack of upwinding. This can be remedied by using SUPG methods which add upwinding by choosing test functions of the form $\eta + \beta\partial\eta/\partial x$ where $\eta$ is a standard shape function. The parameter $\beta$ is adjusted to optimize the accuracy of the numerical scheme. SUPG methods are used extensively for convection-dominated problems in the time domain, see for instance [9]. It is not so common for time-harmonic problems, one exception being the work of Rao and Morris on a finite element model for the linearized Euler equations [6, 7]. In the present work the SUPG test function is written in a form similar to the material derivative:

$$\frac{\mathrm{d}_\alpha\eta}{\mathrm{d}t} = \mathrm{i}\omega\eta + \alpha\frac{\partial\eta}{\partial z}\,.$$

The value of the coefficient $\alpha$ is chosen so that the discretization of the material derivative $\mathrm{d}_0/\mathrm{d}t$ is accurate.

$$\int_\Gamma \overline{\frac{\mathrm{d}_\alpha\sigma_1}{\mathrm{d}t}}\left(v_1 - \frac{\mathrm{d}_{01}\xi}{\mathrm{d}t}\right) + \overline{\frac{\mathrm{d}_\alpha\sigma_2}{\mathrm{d}t}}\left(v_2 - \frac{\mathrm{d}_{02}\xi}{\mathrm{d}t}\right)\mathrm{d}\Gamma$$
$$+ \int_\Gamma \overline{W_1}v_1 - \overline{W_2}v_2 + \overline{\frac{\mathrm{d}_\alpha\eta}{\mathrm{d}t}}\left(\rho_{01}\frac{\mathrm{d}_{01}\phi_1}{\mathrm{d}t} - \rho_{02}\frac{\mathrm{d}_{02}\phi_2}{\mathrm{d}t}\right)\mathrm{d}\Gamma$$

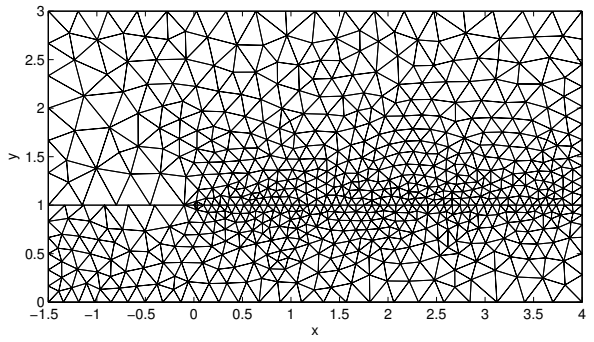


Figure 2: Example of finite element mesh used for the validation.

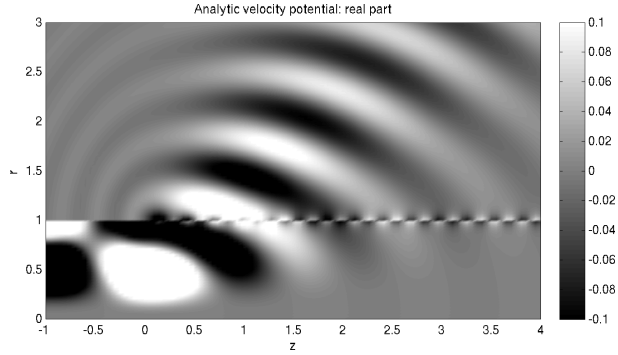


Figure 3: Analytical solution for the velocity potential (real part).

where standard shape functions are used for the test functions $\xi$, $\sigma_1$and $\sigma_2$.

# 4 Validation

## 4.1 Uniform mean flows

We begin by presenting results for the case where the mean flow is uniform. As explained above, even in this case a vortex sheet model is required to describe the vorticity shedding appropriately. We consider a test case based on non-dimensional parameters (using $R$, $c_0$ and $\rho_0$ as reference values). The mean flow Mach number is 0.45 and the Helmholtz number is 10. The sound speed and mean density are uniform. The incident mode is the second radial mode with $m = 3$. The computational domain is shown in Figure 1. The physical region is located within $-1 < z < 3$ and $0 < r < 3$ and is surrounded by a Perfectly Matched Layer to act as a non-reflecting condition (for details of the PML implementation see [2]). An example of the mesh used is given in Figure 2. The element size is slightly reduced along the vortex sheet to better represent the hydrodynamic oscillations.

Figure 3 shows the analytical solution for the velocity potential in the near field. One can observe the acoustic mode radiating from the duct at approximately 50°. Of particular importance here is the presence at $r = 1$, $z > 0$ of the vorticity shed from the trailing edge. Since the acoustic wave and the shed vorticity are coupled at the trailing edge, one has to resolve both accurately.

We begin by considering the convergence of the finite element solution towards the analytical model. This is done in terms of relative error on the velocity potential in the computational domain:

$$\left(\int_\Omega |\phi - \phi_{ex}|^2 \, \mathrm{d}\Omega / \int_\Omega |\phi_{ex}|^2 \, \mathrm{d}\Omega\right)^{1/2},$$

where $\phi_{ex}$ is the exact solution. This is shown in Figure 4 as a function of the mesh resolution. Only the proposed formulation is able to converge towards the expected solution (the plateau observed at a level of error of 0.05% is due to the PML).

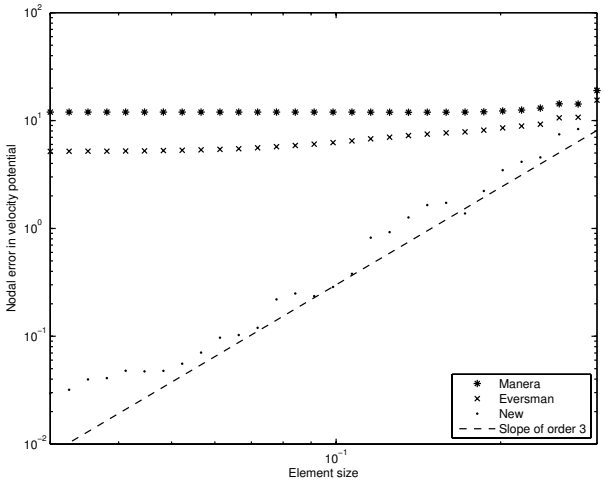


Figure 4: Relative numerical error in % as a function of the mesh resolution.

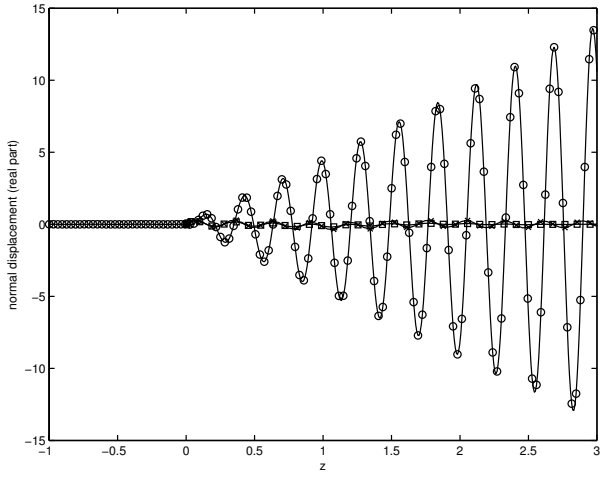


Figure 5: Displacement of the vortex sheet (real part). Analytical solution (∘), Eversman and Okunbor (□), Manera *et al.* (×).

To better explain these observations we now consider the displacement of the vortex sheet. The numerical results are compared against the analytical solution for the existing and new formulation in Figures 5 and 6, respectively. It is clear that the previous formulations of the vortex sheet are not able to capture the hydrodynamic oscillations which are strongly underestimated. The proposed formulation captures these oscillations accurately. It is shown in Figure 6 that the SUPG method is crucial in achieving this.

In addition, we can compare the sound fields away from the vortex sheet as shown in Figure 7. The differences between the formulation of Manera *et al.* and the analytical

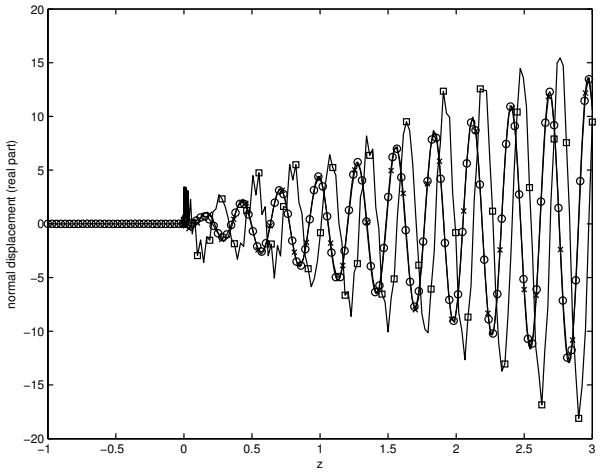


Figure 6: Displacement of the vortex sheet (real part). Analytical solution (∘), new formulation without SUPG (□) and with SUPG (×).

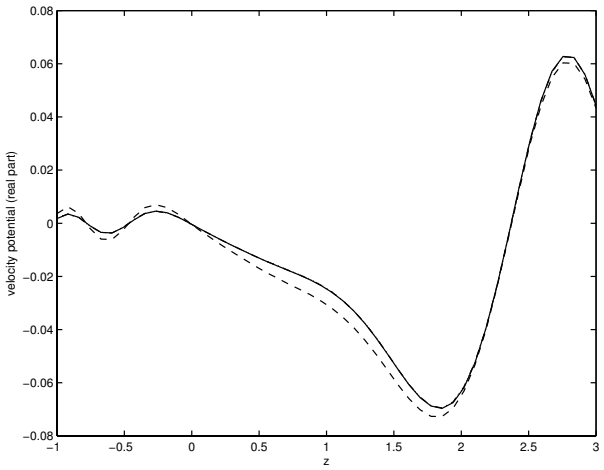


Figure 7: Velocity potential (real part) at $r = 2.75$ for a mesh resolution of 0.1. Analytical solution (solid line), Eversman & Okunbor (dot-dashed line), Manera *et al.* (dashed line) and the new formulation (dotted line).

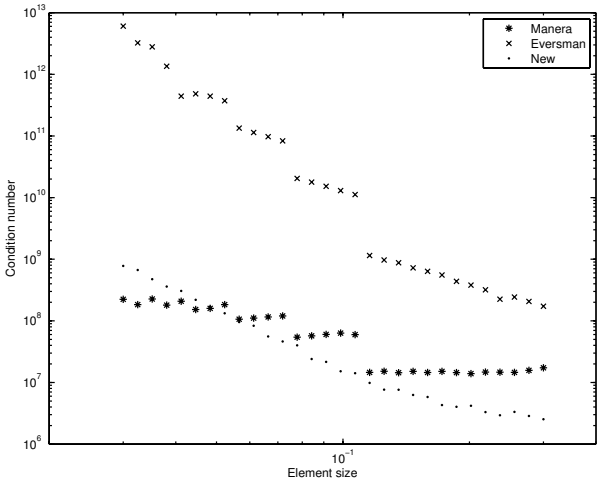


Figure 8: Condition number as a function of the mesh resolution.

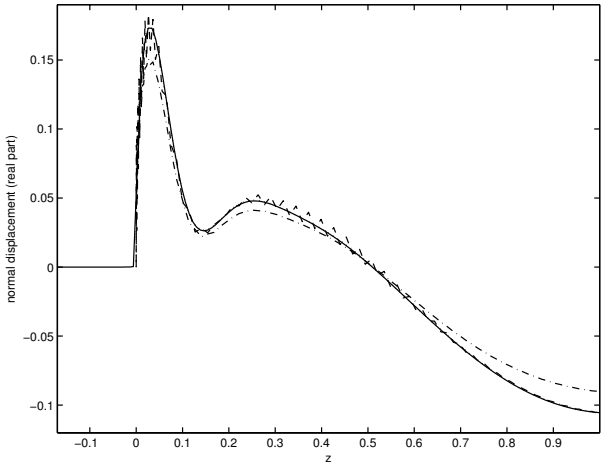


Figure 9: Displacement of the vortex sheet (real part) for the case with non-uniform flow: Analytical solution (solid line), Eversman & Okunbor (dot-dashed line), Manera *et al.* (dashed line) and the new formulation (dotted line).

solution are visible. However, the formulation proposed by Eversman & Okunbor agrees quite well with the theory. This is because this formulation imposes the continuity of velocity which is valid in the special case of a uniform flow. So, even though it doesn't capture the vorticity shedding accurately it can still provide a valid prediction of the acoustic field in this case.

Finally, Figure 8 presents the condition number of the numerical model. This is particularly important to assess since the conditioning of the linear system greatly influences the rate of convergence of iterative solvers. It can be seen that the conditioning of the proposed formulation compares quite well with the other two formulations.

## 4.2 Non-uniform mean flows

For the case with non-uniform flow we consider a Mach number of 0.45 for the jet and 0.1 for the ambient flow (the mean density and sound speed remain uniform). It should be noted that the vortex sheet is unstable and supports a Kelvin-Helmholtz instability, but that solving this kind of problem in the frequency domain generally yields a non-causal solution which doesn't include the instability wave. We will discuss the case where the Kutta condition is not enforced at the trailing edge (the case with the Kutta condition is still under investigation).

Figure 9 shows the displacement of the vortex sheet. The formulation proposed by Eversman & Okunbor does not yield the correct solution. This is to be expected since the continuity of normal velocity that is imposed across the vortex sheet does not apply in this case. The formulation of Manera *et al.* tends to follow the analytical solution but exhibits node-to-node oscillations. Finally, the new formulation does not produce such oscillations and matches the analytical model very well.

Figure 10 shows the velocity potential outside the jet on the line $r = 2.75$. As for the vortex sheet displacement, the formulation by Eversman & Okunbor yields a solution different from the analytical model. The other three solutions agree relatively well.

All of these observations are confirmed by Figure 11, which shows the convergence of the numerical models as the mesh resolution is increased. It is clear that the formulation of Eversman & Okunbor does not convergence to the appropriate solution. The new formulation converges towards the

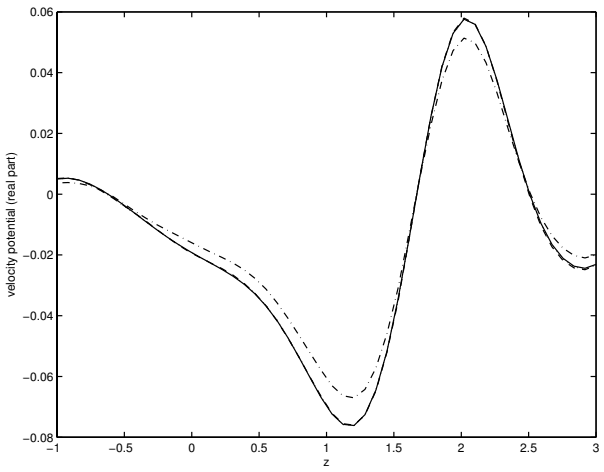


Figure 10: Velocity potential (real part) at $r = 2.75$ for the case with non-uniform flow: Analytical solution (solid line), Eversman & Okunbor (dot-dashed line), Manera *et al.* (dashed line) and the new formulation (dotted line).

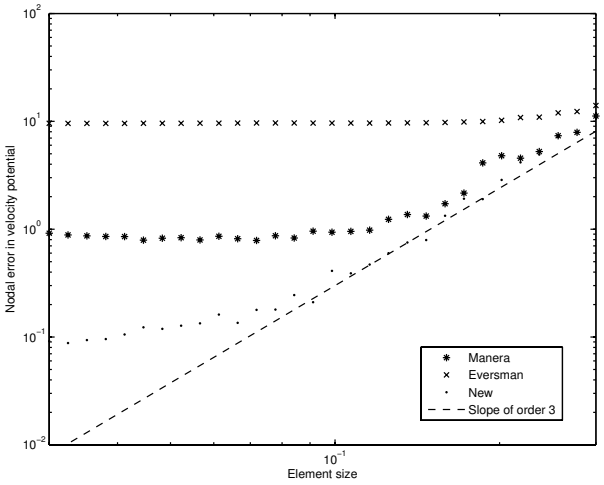


Figure 11: Relative numerical error in % as a function of mesh resolution for the case with a non-uniform flow.

analytical solution (the plateau observed in the error at 0.1% is due to the finite accuracy with which the reference solution is computed). The formulation of Manera *et al.* introduces somewhat larger levels of error. This can be traced back to its inability to capture the oscillations of the vortex sheet as illustrated in Figure 9.

# 5 Conclusions

Two finite element formulations of a vortex sheet have been revisited and validated. A novel formulation has also been proposed. It provides direct control over the behaviour of the solution at the trailing edge (with or without Kutta condition), and it includes a SUPG method to improve the resolution of the hydrodynamic oscillations of the vortex sheet. The formulation proposed by Eversman & Okunbor provides good far-field results for uniform mean flows but cannot yield the correct solution for non-uniform mean flows. In comparison, the formulation by Manera *et al.* can provide accurate solutions for non-uniform flows when the Kutta condition is not enforced, but it is not possible to enforce the Kutta condition.

# Acknowledgments

This project is funded by the Engineering and Physical Sciences Research Council (UK) and LMS International (Belgium).

# References

[1] R.J. Astley. Numerical methods for noise propagation in moving flows, with application to turbofan engines. *Acoustical Science and Technology*, 30(4):227–239, 2009.

[2] A. Bermúdez, L. Hervella-Nieto, A. Prieto, and R. Rodríguez. Perfectly matched layers. In S. Marburg and B. Nolte, editors, *Computational acoustics of noise propagation in fluids – finite and boundary element methods*, pages 167–196. Springer, 2008.

[3] W. Eversman and D. Okunbor. Aft fan duct acoustic radiation. *Journal of Sound and Vibration*, 213(2):235–257, 1998.

[4] G. Gabard and R.J. Astley. Theoretical model for sound radiation from annular jet pipes: far- and near-field solutions. *Journal of Fluid Mechanics*, 549:315–341, 2006.

[5] J. Manera, S. Caro, and G. Lielens. Shear layer modelization with a finite element model – variants of the munt problem. In $13^{th}$ *AIAA/CEAS Aeroacoustics Conference*, 2007. AIAA paper 2007-3555.

[6] P.P. Rao. *High order unstructured grid methods for computational aeroacoustics*. Ph.d. thesis, Pennsylvania State University, 2004.

[7] P.P. Rao and P.J. Morris. Use of finite element methods in frequency domain aeroacoustics. *AIAA Journal*, 44(7):1643–1652, 2006.

[8] F. Treyssède and M. Ben Tahar. Jump conditions for unsteady small perturbations at fluid–solid interfaces in the presence of initial flow and prestress. *Wave Motion*, 46:155–167, 2009.

[9] O.C. Zienkiewicz, R.L. Taylor, and P. Nithiarasu. *The finite element method*. Butterworth-Heinemann, 2006.